Annals of Glaciology 33 2001
© International Glaciological Society

Modeling of the Beaufort ice–ocean climatology change

Larissa Nazarenko,[1] Nickolai Tausnev[2]
[1]*Center for Climate Systems Research, NASA Goddard Institute for Space Studies, Columbia University, New York, NY 10025, U.S.A.*
[2]*Rutgers University, NASA Goddard Institute for Space Studies, New York, NY 10025, U.S.A.*

ABSTRACT. A coupled ice–ocean model is used to study the sensitivity of the Beaufort Sea climatology to representation of sub-grid-scale eddies; to hypothetically not present and double Mackenzie River discharge; and to approximate climate warming specified through a surface air-temperature increase of 3°C. The eddy effect is considered in two ways: as eddy interaction with sea-floor topography yielding a driving force ("neptune" parameterization) and as eddy diffusion and viscosity. The model with neptune parameterization reproduces surface layer circulation, as well as the bathymetrically steered Beaufort Undercurrent, while the model with usual damping does not simulate the Beaufort Undercurrent. The absence of the strong boundary Beaufort Undercurrent affects the thermohaline structure of the Beaufort Sea which becomes less consistent with observational data. The increase of the Mackenzie River discharge causes more northward transport of sea ice, resulting in sea-ice thinning in Mackenzie Bay, while the absence of the Mackenzie River discharge induces southward sea-ice drift and sea-ice thickening in Mackenzie Bay. The sensitivity study of surface air-temperature warming shows a shrinkage of sea ice by 6% in area and 15% in volume, causing the freshening and warming of the surface ocean layer. The sensitivity studies of river discharge and surface air temperature use the neptune parameterization.

INTRODUCTION

Knowledge of the ice regime and water properties of the Beaufort Sea is of general scientific interest and of engineering importance for petroleum development. The ice conditions are defined by the interactions between the atmosphere, the sea ice and the ocean and involve the transfer of momentum, heat and fresh water. Momentum is passed from the atmosphere to the ice or ocean by wind stress, and partitioned between the ice and the ocean. Heat is also transferred between the atmosphere and the ice or the ocean. Fresh water may pass between the ice or ocean and the atmosphere through precipitation, evaporation or sublimation. It is also passed from the ocean to the ice when ice freezes, or from the ice to the ocean during ice melt. Inputs of fresh water to the shelves by river inflow increase the stability of Arctic surface water, thereby promoting winter ice growth and suppressing deep convection.

In addition to the petroleum development, there is huge scientific interest in the global warming phenomenon that has been studied in many numerical models (Washington and Meehl, 1984; Schlesinger and Mitchell, 1987; Gordon and Hunt, 1994; Cattle and Crossley, 1995; Hansen and others, 1997; Randall and others, 1998). Major changes in Arctic climate will cause changes in the sea-ice cover, as well as in other ocean components. Another possible consequence of atmospheric warming is a change in the discharge from the Mackenzie River, the fourth largest river entering the Arctic Ocean, which may affect the ocean circulation, temperature, salinity and sea-ice cover.

Previous simulation studies of the Beaufort Sea include the ice-only models by Coon (1980), Pritchard (1984), Ross (1984) and Yao and others (1992), and a time-dependent, one-dimensional model for the Mackenzie shelf/estuary by Omstedt and others (1994). Coon (1980) reviewed the development of the Arctic Ice Dynamics Joint Experiment (AIDJEX) model of the dynamics and thermodynamics of sea ice. The goal of the AIDJEX modeling was to develop an understanding of the dynamics and thermodynamics of sea ice, on a space of 100 km and a time-scale of 1 day. Pritchard (1984) used the free-drift ice model to simulate ice motions in the Beaufort Sea, and compares these with motions observed during AIDJEX. Quantitative comparisons between the simulated and observed motions were used to verify the accuracy of the model. The dynamic–thermodynamic Hibler (1979, 1980) model was used by Ross (1984) to examine sea-ice thickness fields in the Beaufort Sea and to investigate the potential of ice thickness as a predictor of summer ice conditions. The results of this simulation support the conclusion of Rogers (1978) that atmospheric fluctuations become progressively more important throughout the summer in affecting ice conditions in the Beaufort Sea. Yao and others (1992) described results of a comprehensive study designed to develop a verification system for regional sea-ice models. The system is used to evaluate model performance of several model forecast outputs, including ice velocity, total and partial (by ice types) concentrations and ice-edge location. Sensitivity studies with a one-dimensional model for the Mackenzie shelf/estuary by Omstedt and others (1994) show that the fresh-water content of the Mackenzie shelf/estuary is highly influenced by freezing, ice advection off the shelf and wind-driven transport, all of which remove fresh water from the shelf. The high-resolution Arctic model of Zhang and others (1999) has been used for ocean and ice simulations where the Beaufort Sea is presented on a grid of 18 km. Their results show that the Beaufort Gyre can be reduced in size due to anomalous atmospheric circulation. Ocean eddies can be a major contributor to mesoscale reduction of ice concentration, in addition to atmos-

https://doi.org/10.3189/172756401781818491 Published online by Cambridge University Press

pheric storms which usually lead to a broad-scale reduction of ice concentration.

The model used in this regional study is a three-dimensional coupled ice–ocean model, where we address and solve the open-boundary problem. The inclusion of parameterization of eddy interaction with sea-floor topography is required because of the inability of the model to solve the small-scale Arctic eddies. Inclusion of the Mackenzie River discharge plays an important part in changing the cycle of fresh-water inflow in the Mackenzie Bay area. The dynamic–thermodynamic sea-ice model (Hibler, 1979; Parkinson and Washington, 1979) includes calculation of snow cover, as well as transformation of snow into ice (Oberhuber and others, 1993). This coupled ice–ocean model can be used for any region of the ocean with ice cover.

The objectives of this study are (1) to examine the influence of the increased and decreased Mackenzie River discharges on sea-ice and ocean circulation, temperature and salinity, and (2) to investigate the impact of surface air-temperature warming on sea-ice conditions and ocean thermohaline structure. Furthermore, we compare two different methods of small-scale eddy representation: consideration of eddy interaction with sea-floor topography as a driving force (Holloway, 1992), and parameterization of eddy effects as eddy diffusion and viscosity. The sensitivity studies of the Mackenzie River discharge and surface air-temperature warming use the "neptune" parameterization.

COUPLED MODEL

The model used in this study is a coupled ice–ocean model (Nazarenko and others, 1997). The lateral horizontal kinematic eddy viscosity and diffusion constants are $10^5\,\mathrm{m^2\,s^{-1}}$ and $10^3\,\mathrm{m^2\,s^{-1}}$, respectively, and vertical eddy viscosity and diffusion coefficients are $10^{-3}\,\mathrm{m^2\,s^{-1}}$ and $5\times10^{-5}\,\mathrm{m^2\,s^{-1}}$, respectively. Snow and ice thickness, compactness and velocity were generated from the dynamic–thermodynamic model developed by Hibler (1979) and Parkinson and Washington (1979), with some modifications for transformation of snow into ice after Oberhuber and others (1993).

Representation of sub-grid eddies is an ongoing research topic which is of special concern in the Arctic where eddies are of relatively small (O(10 km)) horizontal scales (Manley and Hunkins, 1985; Padman and others, 1990). The alternative is to parameterize eddy effects, usually as eddy diffusion and viscosity (or other damping). We have introduced a parameterization (neptune) which considers the role of eddies interacting with bottom topography, yielding a driving force (rather than damping) applied to the model-resolved flows. The theoretical basis for neptune is discussed by Holloway (1987, 1992, 1996), with practical implementation described in Alvarez and others (1994). Horizontal velocities u and v in the horizontal viscosity operator were replaced with $u-u^*$ and $v-v^*$ (equations (6) and (7) in Nazarenko and others, 1998), where u^* and v^* were obtained from the stream function $\psi^*=-fL^2H$, where H is bottom topography, f is the Coriolis parameter and L^2 is a parameter characterizing a horizontal scale in eddy vorticity. In practice, Eby and Holloway (1994) have prescribed L to vary from 3 km at the North Pole to 12 km at tropical latitudes. We have simply assumed constant $L=4$ km to characterize the Beaufort domain.

Most sea-ice forecasting models have been developed to minimize open-boundary problems by simulations over a large region, for example, the whole Arctic basin. For the present purpose, this approach significantly increases computation load, as the Arctic basin is almost six times larger than the Beaufort Sea. To save computation we develop a coupled model with boundary conditions suitable for application to the Beaufort Sea. The domain chosen for this study includes the Beaufort Sea and Amundsen Gulf. The model bathymetry is obtained by interpolating the ETOPO5

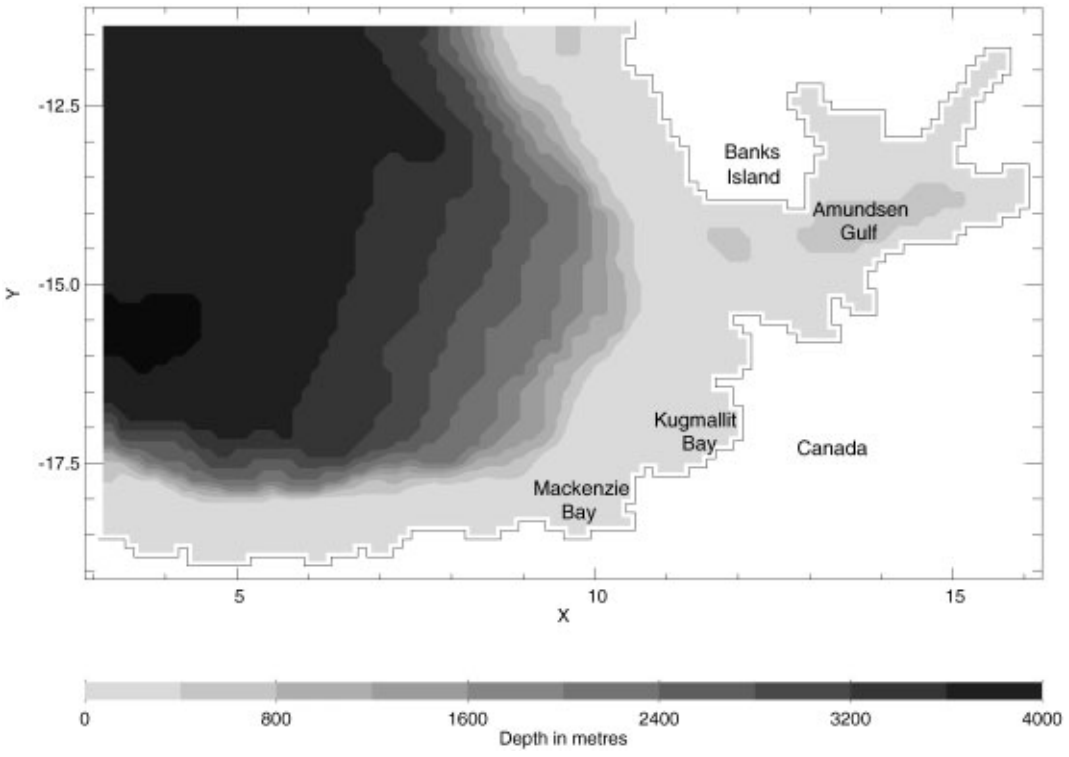

Fig. 1. Model bathymetry. The grey-scale interval is 400 m.

https://doi.org/10.3189/172756401781818491 Published online by Cambridge University Press

(1986) bottom topographic dataset onto the model grid (Fig. 1). Horizontal resolution is approximately 15 km, with 24 levels in the vertical covering 4080 m in depth intervals from 20 m at the surface to 390 m at the deep ocean.

For inflow on the open boundary, we specify temperature and salinity from monthly mean Levitus (1982) data; baroclinic velocities are specified as calculated geostrophic velocities using monthly mean Levitus (1982) temperature and salinity; barotropic velocities are specified from monthly output from the larger Arctic model (Nazarenko and others, 1997), enhanced by a locally determined neptune stream function taking account of finer-scale resolution of topographic features. For outflow on the open boundary, we apply linear interpolation between interior temperature and salinity and monthly mean Levitus (1982) data according to the velocity normal to the open boundary. The same techniques were implemented for baroclinic velocities on the open boundary. This technique for the outflow condition has been chosen experimentally to avoid the disturbances induced by specified open boundaries.

Both Hibler (1979) and Zhang and Hibler (1997) treated the boundary as a zero-sea-ice velocity Dirichlet condition. For the open boundary they set the ice strength to zero. This approximation is successful for simulations over the whole Arctic, in which case open boundaries occur only in limited areas like the Bering Strait, Fram Strait or Greenland and Norwegian Seas. However, for simulations in a sub-area of the Arctic, like the Beaufort Sea, this open-boundary approximation is inappropriate. To solve this problem we implement the Von Neumann boundary condition for ice velocity:

$$\frac{\partial \vec{V}}{\partial \vec{n}} = 0\,, \qquad (1)$$

where $\vec{n}$ is along the direction normal to the boundary. The open-boundary values for ice thickness and concentration we specify in the same way as the ocean model variables.

According to annual mean values over about 20 years, the fresh-water discharge from Mackenzie River varies from 3220 $m^3\,s^{-1}$ in winter months to 21 102 $m^3\,s^{-1}$ in summer (Marsh and Prowse, 1993). In summer the Mackenzie River discharges about 75% of its annual inflow. The fresh-water flux from Mackenzie is specified as negative salinity flux on the ocean surface. On the distance of 20 gridpoints from the river mouth, we assume that the fresh-water outflow is 10 times smaller.

Atmospheric forcing (monthly climatological fields of wind stress, surface air temperature, humidity, radiation and heat fluxes) is supplied by datasets or bulk formulae. European Centre for Medium-range Weather Forecasts (ECMWF) 2 m air temperatures and dew-point temperatures for 1986–92 are available as a part of the Sea Ice Model Intercomparison Project (Lemke and others, 1997). The ECMWF wind field for 1986–92 is averaged to monthly climatological means (Trenberth and others, 1989). Atmospheric humidity, shortwave, longwave, sensible- and latent-heat fluxes were calculated using bulk formulae.

Where the ice is not present, we combine atmospheric forcing (Lemke and others, 1997) and restoring conditions for surface temperature using climatological values (Levitus, 1982), and fresh-water flux for surface salinity from the Mackenzie River discharge. We restore the surface ocean temperature over 25 m depth with a time-scale of 30 days. For partially ice-covered gridcells, the surface boundary conditions contain partly the heat flux through leads and

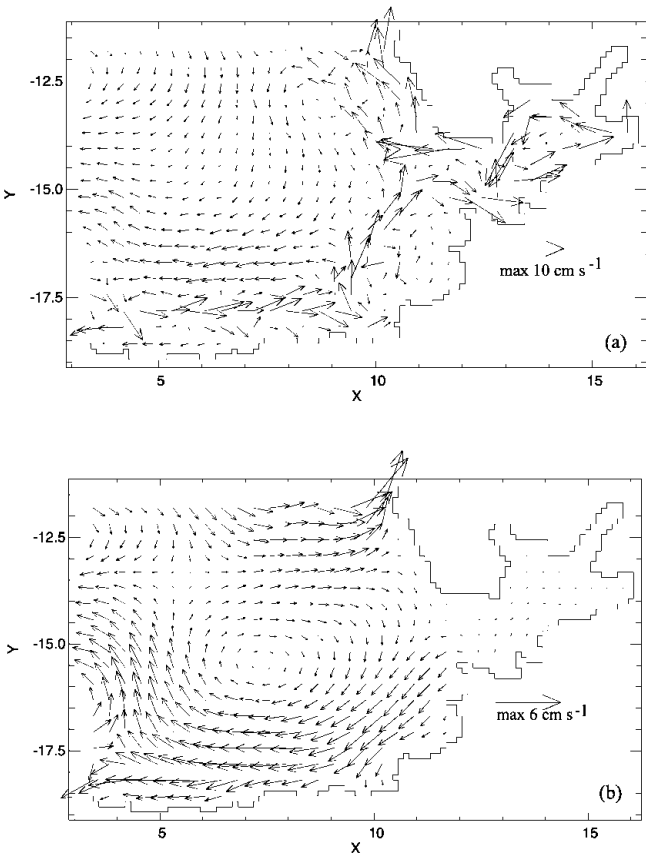

Fig. 2. Velocity fields at 30 m for December, with (a) and without (b) neptune parameterization.

ice conduction computed in the ice model and partly the restoring towards the climatology for surface temperature, and also the salt-water/fresh-water flux from ice growth/melt and fresh-water Mackenzie outflow for the surface salinity.

Integration was started from zero velocity, no ice and annual mean Levitus (1982) temperature and salinity. The ocean model was integrated under monthly-varying forcing with restoring to Levitus (1982) as a boundary condition until quasi-equilibrium was attained at upper and intermediate depths. There was no ice model for the first 40 years of ocean spin-up. After quasi-equilibrium was attained, an ice model was included. The acceleration method of Bryan (1984) was used with this time-dependent forcing. For the ocean and ice models the time-step was 3 hours. The coupled ice–ocean model was integrated for 20 more years. The changes of the volume mean temperature and salinity are about 2×10^{-4} °C and 4×10^{-5} ppt during the last year of integration. The change of area mean ice thickness is 3×10^{-4} m during the last year of integration.

After 20 year integration of the coupled ice–ocean model, four additional 10 year experiments were conducted. The first examined the role of neptune in the circulation, temperature and salinity structures, as well as in sea-ice conditions. The next two experiments (with no and double river discharge) explored the influence of the Mackenzie River discharge on sea ice and ocean even though the freezing temperature of sea water is not dependent on salinity. The last experiment considered the effect of surface air-temperature warming on the sea-ice state, as well as on the ocean thermohaline structure in the Beaufort Sea. For this purpose a year-round constant 3°C warming was chosen and sustained for 10 year integration.

https://doi.org/10.3189/172756401781818491 Published online by Cambridge University Press

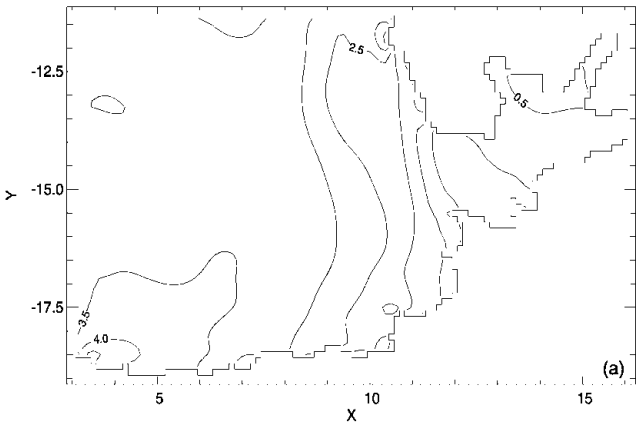

Fig. 3. Ice-thickness fields (neptune parameterization case) for (a) January, (b) July. Contour interval is 0.5 m.

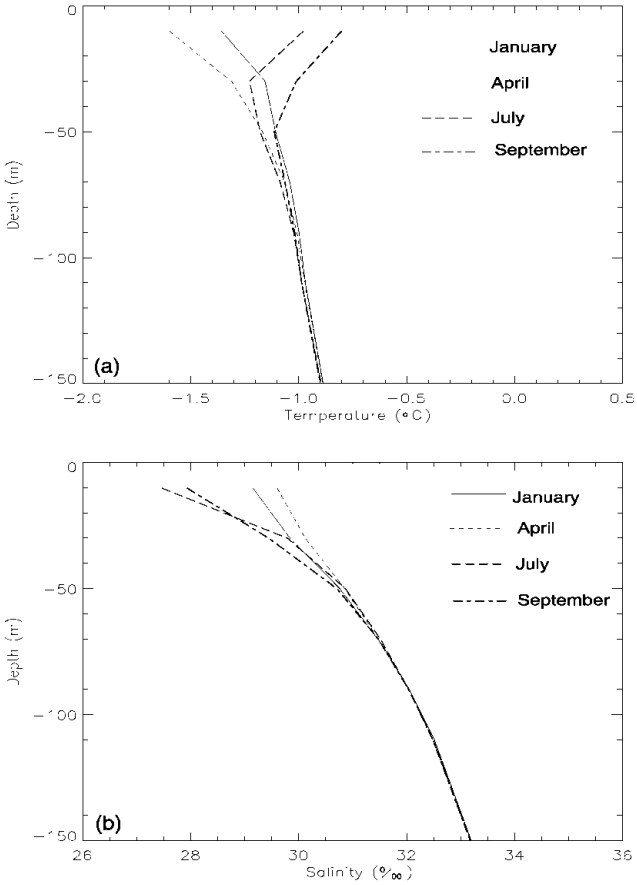

Fig. 4. Vertical profiles (neptune parameterization case) of (a) temperature, (b) salinity.

RESULTS

Neptune and no-neptune experiments

Analysis of results with and without neptune parameterization showed that the model with neptune reproduced the Arctic Ocean circulation more consistently with observations (Nazarenko and others, 1997). Both models reproduce the largest persistent feature of the surface and near-surface circulation, the Beaufort Gyre, which is associated with a clockwise circulation (Fig. 2a and b). Another conspicuous feature of the Beaufort Sea circulation is the Beaufort Undercurrent which follows the bottom contours to the east (Aagaard, 1984). The model without neptune does not reproduce this feature (Fig. 2b), whereas circulation from the model with neptune includes the bathymetrically steered eastward flow (Fig. 2a). This current extends seawards from the 30–50 m isobaths to the base of the continental slope and increases with depth. This relatively strong deep-reaching boundary current is part of the large-scale circulation of the Canadian Basin of the Arctic Ocean (Nazarenko and others, 1997). The strong, narrow Beaufort Undercurrent brings the colder, saltier water at the surface, and warmer, saltier water at intermediate depths, into the Beaufort Sea from the Chukchi Sea. Since the surface temperature is colder, the model with neptune simulates the thicker sea ice in the Alaskan shelf (not shown). The intermediate ocean layer is colder and less saline in the model without neptune, due to the absence of the Atlantic warm-water inflow from the Chukchi Sea.

Because the surface and intermediate water circulation reproduced by the model with neptune is more consistent with observations (Aagaard, 1984), we used this model for the following experiments. The seasonal variations of modeled surface temperature and sea-ice concentration and thickness are coherent. The warmest surface water is +2.7°C in the Amundsen Gulf in July. The warming of the surface water on the continental shelf starts in May and continues until August. Ice melting begins in the Amundsen Gulf in April, and by the end of May it is mostly ice-free and only the northern part is still ice-covered. The largest ice-free area in the Beaufort Sea occurs in July (Fig. 3b). In the central part of the Beaufort Sea the multi-year ice is thinner in July than in January (Fig. 3a and b). Gradual cooling takes place from August. The temperature of the surface water in the Amundsen Gulf reaches −0.6°C in April. The temperature of the surface water under the pack ice is little influenced by seasonal changes, and remains equal to approximately freezing temperature, −1.8°C. Ice growth starts in September, and the latest ice forms in the Amundsen Gulf at the end of September. Ice growth continues throughout winter.

Analysis of the vertical profiles of horizontal averaged temperature and salinity (Fig. 4a and b) shows the results of both decreased fresh-water input and increased salinity due to ice formation. The freezing process also results in convective mixing within and thickening of the surface layer. As the ice thickens, its growth rate decreases due to decreased heat flux through it. As a result, the layer immediately under the ice is up to 40 or 50 m deep, with a negative thermocline and halocline. The water below this layer is only slightly influenced by seasonal changes; both its temperature and salinity increase with depth.

In contrast, the water column in summer is quite stable.

https://doi.org/10.3189/172756401781818491 Published online by Cambridge University Press

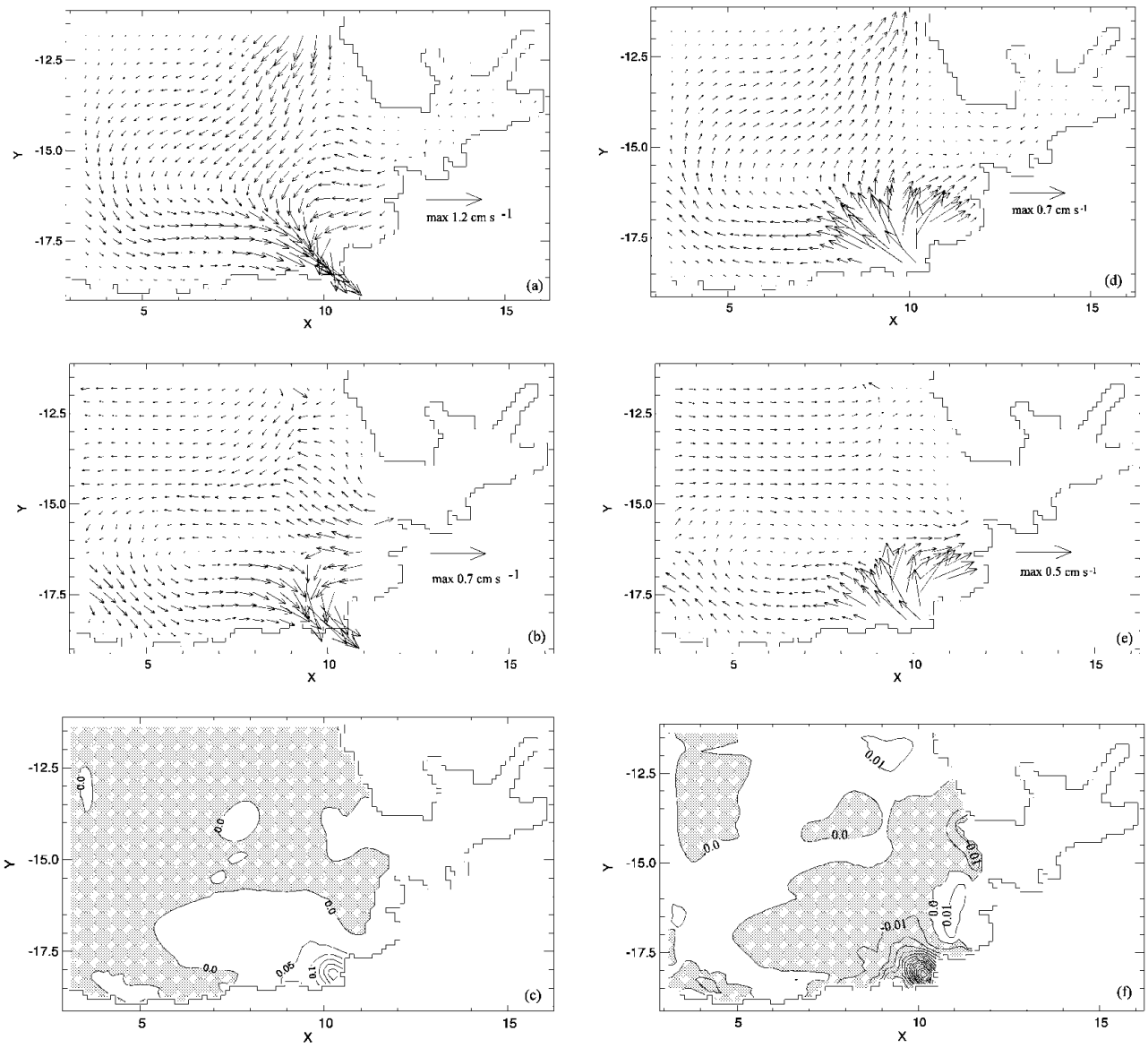

Fig. 5. Differences for June. (a) Velocity at 10 m (no-river case minus control); (b) sea-ice drift (no-river case minus control); (c) sea-ice thickness (no-river case minus control). Contour interval is 0.05 m. (d) Velocity at 10 m (double-river case minus control); (e) sea-ice drift (double-river case minus control); (f) sea-ice thickness (double-river case minus control). Contour interval is 0.01 m.

The input of fresh water from ice melting and from increased river flow, as well as the increase in temperature due to insolation, all act to produce a low-salinity, relatively fresh layer and strong stable stratification. Mixing processes, whether wind- or current-induced, are thus confined to this 40–50 m thick surface layer (Fig. 4a and b).

River runoff experiments

The freezing temperature of sea water does not depend on ocean salinity in our model, so the influence of the Mackenzie River discharge on sea-ice formation cannot be investigated directly. Nevertheless, the tendency in sea-ice change correctly reflects the salinity effect, which can be attributed to the dynamical processes in this model. The model without Mackenzie River discharge reproduces the saltier water in Mackenzie Bay, which becomes heavier than the water masses in the central Beaufort Sea. Currents of the ocean surface layer are directed towards the coast, to replace the denser water by lighter water (Fig. 5a). Circulation of the ocean surface layer directly affects the sea-ice drift (Fig. 5b) that transports more ice to Mackenzie Bay (Fig. 5c). The model with double Mackenzie River discharge displays the opposite picture (Fig. 5d–f). Light, less saline water flows to the central Beaufort Sea from Mackenzie Bay. Sea-ice drift follows the surface layer currents and transports sea ice to the central Beaufort Sea, and the sea-ice thickness is therefore reduced. The inclusion of salinity dependence of ocean freezing temperature might be the next step for improving this model.

Climate-warming experiment

Satellite observations and historical records show a decrease in Northern Hemisphere sea-ice extent during the past 46 years (Maslanik and others, 1996; Cavalieri and others, 1999; Gloersen and others, 1999; Johannessen, 1999; Parkinson and others, 1999). One reason for sea-ice shrinkage might be global warming due to increased levels of greenhouse gases. Mathematical models have been used in many studies to ascertain the effects of an increase in greenhouse gases on the Earth's climate (Washington and Meehl, 1984; Schlesinger and Mitchell, 1987; Cattle and Crossley, 1995; Hansen and

https://doi.org/10.3189/172756401781818491 Published online by Cambridge University Press

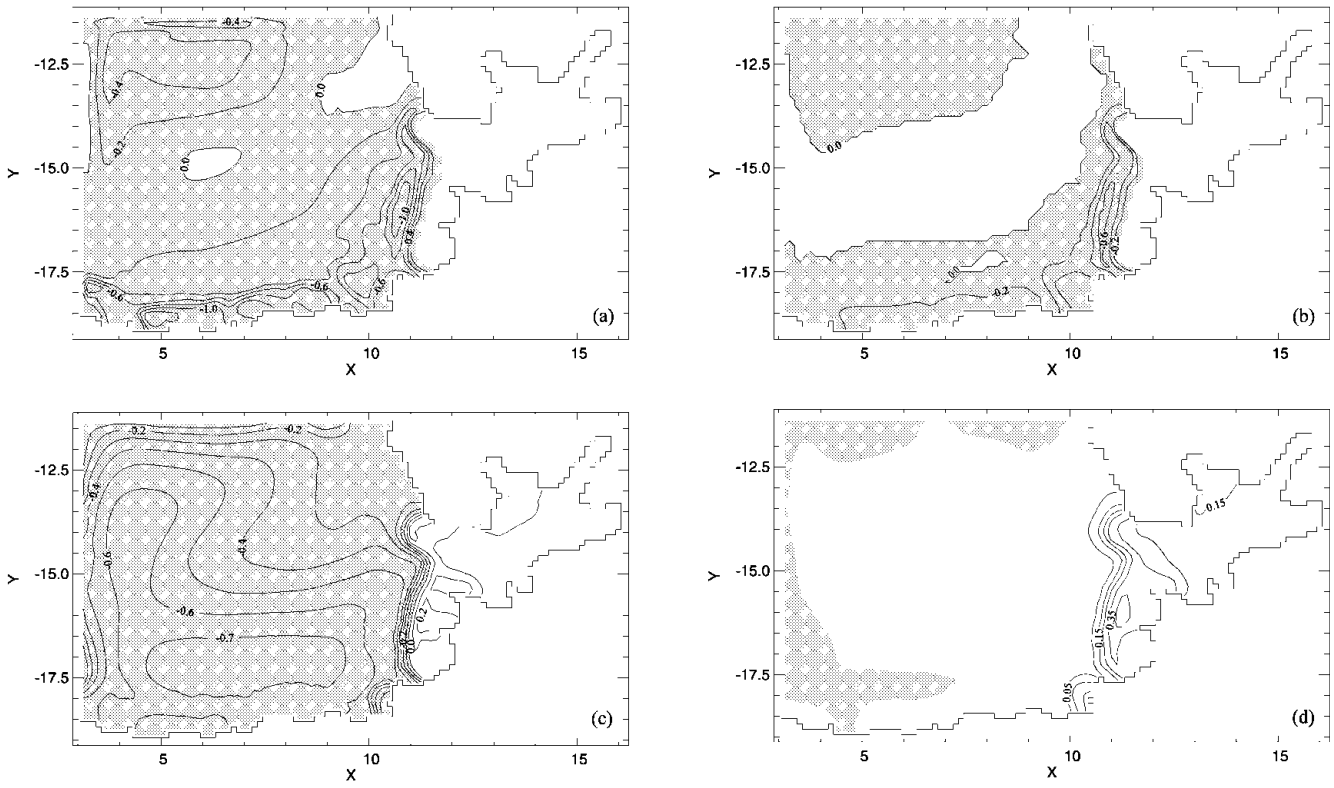

Fig. 6. Differences for 3°C warming case minus control, June: (a) sea-ice thickness (contour interval 0.02 m); (b) sea-ice concentration (contour interval 0.2); (c) salinity at 10 m (contour interval 0.1 ppt); (d) temperature at 10 m (contour interval 0.1°C).

others, 1997). Different models show a 5–10°C increase in surface air temperature in both polar regions.

Although this model does not include an interactive coupling between the atmosphere and the ocean, we conducted an experiment with constant surface air-temperature warming of 3°C. In winter, such an increase is too slight to have much impact on sea-ice state since it does not essentially change heat fluxes into sea ice: sea ice is reduced by 0.3% in area and by 1.9% in volume. In summer, sea ice is more sensitive to the surface air-temperature increase: it shrinks by 6% in area and by 15% in volume. The largest changes in sea-ice thickness occur around the ice edge, with maximum thinning of 1.4 m (Fig. 6a). Although sea ice thins over the whole Arctic, the extent of multi-year ice does not change in the central Beaufort Sea. Most changes of sea-ice extent take place around the ice edge (Fig. 6b). The sea-ice melting affects the salinity of the Beaufort Sea, with an average overall freshening by 0.5 ppt for the surface layer (Fig. 6c). Sea ice provides a good isolation for the ocean surface layer even though the sea-ice thickness has reduced. Nevertheless, the model reproduces a slight warming of the first ocean layer in the central Beaufort Sea, with a maximum ocean temperature increase of 0.5°C close to the sea-ice margin (Fig. 6d). Although the sensitivity of this model is weak because of the absence of the atmosphere–ice–ocean interaction, the tendency of ice–ocean changes is consistent with observations (Johannessen and others, 1999). Johannessen and his colleagues found that the area of multi-year ice declined by 7% per decade from 1978 to 1998.

CONCLUSION

A coupled ice–ocean model is used for simulating the Beaufort ice–ocean climatology, as well as for sensitivity studies of the Beaufort ice–ocean conditions to represent sub-grid-scale eddies, no and double Mackenzie River discharges and surface air-temperature warming. Sensitivity studies and control simulation show the relative importance of the physical processes, as well as the areas for possible improvement of the model.

The inclusion of parameterization of eddy interaction with ocean topography is required since the model does not resolve the small-scale Arctic eddies (about 10 km). Comparison of ocean circulation from models with and without neptune parameterization shows that the model without neptune failed to reproduce the Beaufort Undercurrent, the strong bathymetrically steered boundary current that is part of the large-scale circulation of the Arctic Ocean. In the absence of the Beaufort Undercurrent, the surface ocean layer is warmer and less saline along the Alaskan coast in the model without neptune, causing less sea-ice formation on the Alaskan shelf.

Since the circulation of surface and intermediate layers in the model with neptune is more consistent with observations, we used this model for other sensitivity studies. Although ocean freezing temperature does not depend on salinity, the model reproduces the response of sea ice to the modification of the Mackenzie River discharge that can be featured as a dynamical process. The model without the Mackenzie River discharge displays saltier, heavier water in Mackenzie Bay, and ocean currents towards the coast replace them with lighter water from the central Beaufort Sea. As a result, an increased southward sea-ice drift brings more ice to Mackenzie Bay. The model with the double Mackenzie River discharge shows the opposite picture of sea-ice state and ocean circulation and thermohaline structure. The flows of light, less saline water out of Mackenzie Bay to the central Beaufort Sea induce more northward transport of sea ice that causes thinning of the sea ice in Mackenzie Bay.

https://doi.org/10.3189/172756401781818491 Published online by Cambridge University Press

This model simulates well the sea-ice retreat and thermohaline structure under surface air-temperature warming. The increase of surface air temperature by 3°C has an essential impact on summer sea ice: sea ice is decreased by 6% in area and by 15% in volume. The largest thinning of 1.4 m occurs around the sea-ice edge. Sea-ice melting freshens, while sea-ice shrinkage warms, the surface ocean layer.

This model can be used for rough sensitivity studies, but improvements are possible. One plausible development of the model might be the inclusion of dependence of ocean freezing temperature on salinity. In order to improve the radiative forcing on the snow-ice surface, the parameterization of the surface albedo could be modified.

REFERENCES

Aagaard, K. 1984. The Beaufort undercurrent. *In* Barnes, P.W., D. M. Schell and E. Reimnitz, *eds. The Alaskan Beaufort Sea: ecosystems and environments*. Orlando, FL, Academic Press, 47–71.

Alvarez, A., J. Tintoré, G. Holloway, M. Eby and J.M. Becker. 1994. Effect of topographic stress on the circulation in the western Mediterranean. *J. Geophys. Res.*, **99**(C8), 16,053–16,064.

Bryan, K. 1984. Accelerating the convergence to equilibrium of ocean–climate models. *J. Phys. Oceanogr.*, **14**(7), 970–985.

Cattle, H. and J. Crossley. 1995. Modelling Arctic climate change. *Philos. Trans. R. Soc. London, Ser. A*, **352**(1699), 201–213.

Cavalieri, D. J., C. L. Parkinson, P. Gloersen, J. C. Comiso and H. J. Zwally. 1999. Deriving long-term time series of sea ice cover from satellite passive-microwave multisensor data sets. *J. Geophys. Res.*, **104**(C7), 15,803–15,814.

Coon, M. D. 1980. A review of AIDJEX modeling. *International Association of Hydrological Sciences Publication* 124 (Symposium at Seattle 1977 — *Sea Ice Processes and Models*), 12–27.

Eby, M. and G. Holloway. 1994. Sensitivity of a large-scale ocean model to parameterization of topographic stress. *J. Phys. Oceanogr.*, **24**(12), 2577–2588.

ETOPO5. 1986. *Global 5′ × 5′ depth and elevation*. Boulder, CO, U.S. Department of Commerce. NOAA, National Geophysical Data Center. (Code E/GC3.)

Gloersen, P., C. L. Parkinson, D. J. Cavalieri, J. C. Comiso and H. J. Zwally. 1999. Spatial distribution of trends and seasonality in the hemispheric sea ice cover: 1978–1996. *J. Geophys. Res.*, **104**(C9), 20,827–20,835.

Gordon, H. B. and B. G. Hunt. 1994. Climatic variability within an equilibrium greenhouse simulation. *Climate Dyn.*, **9**(4–5), 195–212.

Hansen, J. *and 42 others*. 1997. Forcing and chaos in interannual to decadal climate change. *J. Geophys. Res.*, **102**(D22), 25,679–25,720.

Hibler, W. D., III. 1979. A dynamic thermodynamic sea ice model. *J. Phys. Oceanogr.*, **9**(7), 815–846.

Hibler, W. D., III. 1980. Modeling a variable thickness sea ice cover. *Mon. Weather Rev.*, **108**(12), 1943–1973.

Holloway, G. 1987. Systematic forcing of large-scale geophysical flows by eddy–topography interaction. *J. Fluid Mech.*, **184**, 463–476.

Holloway, G. 1992. Representing topographic stress for large-scale ocean models. *J. Phys. Oceanogr.*, **22**(9), 1033–1046.

Holloway, G. 1996. Neptune effect: statistical mechanical forcing of ocean circulation. *In* Adler, R. J., P. Muller and B. Rozovskii, *eds. Stochastic modelling in physical oceanography*. Basel, Birkhäuser, 207–220.

Johannessen, O. M., E. V. Shalina and M. W. Miles. 1999. Satellite evidence for an Arctic sea ice cover in transformation. *Science*, **286**(5446), 1937–1939.

Lemke, P., W. D. Hibler, G. Flato, M. Harder and M. Kreyscher. 1997. On the improvement of sea-ice models for climate simulations: the Sea Ice Model Intercomparison Project. *Ann. Glaciol.*, **25**, 183–187.

Levitus, S. 1982. *Climatological atlas of the world ocean*. Rockville, MD, U.S. Department of Commerce. National Oceanic and Atmospheric Administration. (NOAA Professional Paper 13.)

Manley, T. O. and K. Hunkins. 1985. Mesoscale eddies of the Arctic Ocean. *J. Geophys. Res.*, **90**(C3), 4911–4930.

Marsh, P. and T. Prowse. 1993. Hydrologic regime of the Mackenzie Basin, potential modelling approaches, and future research needs for addressing climate change issues. *In Mackenzie basin impact study*. Downsview, Ont., Environment Canada, 37–49. (Int. Report 1.)

Maslanik, J. A., M. C. Serreze and R. G. Barry. 1996. Recent decreases in Arctic summer ice cover and linkages to atmospheric circulation anomalies. *Geophys. Res. Lett.*, **23**(13), 1677–1680.

Nazarenko, L., T. Sou, M. Eby and G. Holloway. 1997. The Arctic ocean–ice system studied by contamination modelling. *Ann. Glaciol.*, **25**, 17–21.

Oberhuber, J. M., D. M. Holland and L. A. Mysak. 1993. A thermodynamic–dynamic snow sea-ice model. *In* Peltier, W. R., *ed. Ice in the climate system*. Berlin, etc., Springer-Verlag, 653–673. (NATO ASI Series I: Global Environmental Change 12.)

Omstedt, A., E. C. Carmack and R.W. Macdonald. 1994. Modeling the seasonal cycle of salinity in the Mackenzie shelf/estuary. *J. Geophys. Res.*, **99**(C5), 10,011–10,021.

Padman, L., M. Levine, T. Dillon, J. Morison and R. Pinkel. 1990. Hydrography and microstructure of an Arctic cyclonic eddy. *J. Geophys. Res.*, **95**(C6), 9411–9420.

Parkinson, C. L. and W. M. Washington. 1979. A large-scale numerical model of sea ice. *J. Geophys. Res.*, **84**(C1), 311–337.

Parkinson, C. L., D. J. Cavalieri, P. Gloersen, H. J. Zwally and J. C. Comiso. 1999. Arctic sea ice extents, areas, and trends, 1978–1996. *J. Geophys. Res.*, **104**(C9), 20,837–20,856.

Pritchard, R. S. 1984. Beaufort Sea ice motions. *In* Barnes, P.W., D. M. Schell and E. Reimnitz, *eds. The Alaskan Beaufort Sea: ecosystems and environments*. Orlando, FL, Academic Press, 95–113.

Randall, D. *and 9 others*. 1998. Status of and outlook for large-scale modeling of atmosphere–ice–ocean interactions in the Arctic. *Bull. Am. Meteorol. Soc.*, **79**(2), 197–219.

Rogers, J. C. 1978. Meteorological factors affecting interannual variability of summertime ice extent in the Beaufort Sea. *Mon. Weather Rev.*, **106**(6), 890–897.

Ross, B. 1984. A model investigation of interannual sea-ice variability in the Beaufort Sea. *J. Glaciol.*, **30**(105), 223–226.

Schlesinger, M. E. and J. F. B. Mitchell. 1987. Climate model simulations of the equilibrium climatic response to increased carbon dioxide. *Rev. Geophys.*, **25**(4), 760–798.

Trenberth, K. E., J. G. Olson and W. G. Large. 1989. *A global ocean wind stress climatology based on ECMWF analyses*. Boulder, CO, National Center for Atmospheric Research. (NCAR Technical Note TN-338+STR.)

Washington, W. M. and G. A. Meehl. 1984. Seasonal cycle experiment on the climate sensitivity due to a doubling of CO_2 with an atmospheric general circulation model coupled to a simple mixed layer ocean. *J. Geophys. Res.*, **89**(D6), 9475–9503.

Yao, T., T. Brown and D. B. Fissel. 1992. *Verification study of sea ice models*. Ottawa, Ont., Environment Canada. Ice Centre. (Report by Arctic Sciences Ltd., Sidney, B.C.)

Zhang, J. and W. D. Hibler, III. 1997. On an efficient numerical method for modeling sea ice dynamics. *J. Geophys. Res.*, **102**(C4), 8691–8702.

Zhang, Y., W. Maslowski and A. J. Semtner. 1999. Impact of mesoscale ocean currents on sea ice in high resolution Arctic ice and ocean simulations. *J. Geophys. Res.*, **104**(C8), 18,409–18,429.

https://doi.org/10.3189/172756401781818491 Published online by Cambridge University Press